13. D. J. Carlson and R. F. Hoglund, "Particle drag and heat transfer in rocket nozzles," AIAA J., 2, No. 11 (1964).
14. A. I. Zhmakin and A. A. Fursenko, "One class of monotonic difference methods of through computing," Zh. Vychisl. Mat. Mat. Fiz., 20, No. 4 (1980).
15. A. A. Gubaidulin, A. I. Ivandaev, and R. I. Nigmatulin, "Modified 'coarse-particle' method for calculation of nonsteady wave processes in multiphase media," Zh. Vychisl. Mat. Mat. Fiz., 17, No. 6 (1977).

TWO-PHASE BOUNDARY LAYER WITH AN INCOMPRESSIBLE CARRIER PHASE ON A PLATE, WITH INJECTION AND SUCTION OF GAS FROM THE SURFACE

A. M. Grishin and V. I. Zabarin

UDC 532.529

Two-phase flows in a boundary layer around bodies of different shapes were examined theoretically in [1-3]. Equations of a two-phase boundary layer were obtained in [1] in four characteristic cases on the basis of asymptotic analysis of the system of equations of two-phase flow at high Reynolds numbers. The structure of a boundary layer with an incompressible carrier phase on the impermeable, stationary surface of a plate was studied in [2]. The investigation [3] examined the effect of the boundary layer on particle trajectory in the flow of an incompressible gas about a sphere in the "single-particle" regime.

Here, we numerically study flow in a two-phase boundary layer about a plate with injection and suction of gas from the surface. An asymptotic analysis of the initial equations of motion of the two-phase medium at high Reynolds numbers produces the boundary condition for the transverse component of particle velocity on the external boundary of the boundary layer.

It was found that the presence of gas suction eliminates the high-particle-density layer in the boundary layer and leads to restructuring of the qualitative flow pattern. An addition is made to the friction coefficient due to particle flow on the surface. With injection of gas from the surface, a layer of pure gas is formed near the surface, while a surface of parameter discontinuity – a sheet – is formed inside the boundary layer.

1. Formulation of the Problem. Written below are the equations of laminar motion of a two-phase mixture in a boundary layer near a flat plate parallel to the incoming flow. We assume that the volume fraction of the chemically inert spherical particles is small, the process is isothermal, there is a small difference between the local characteristics and the mean-volume characteristics, the physical density of the particles is much greater than the density of the carrier phase, Brownian motion of the particles is insignificant, and the Mach numbers are small. The equations of motion in this case have the form [1]:

$$\frac{\partial u}{\partial x}+\frac{\partial v}{\partial y}=0,\quad \frac{\partial \rho_s u_s}{\partial x}+\frac{\partial \rho_s v_s}{\partial y}=0, \tag{1.1}$$

$$u\frac{\partial u}{\partial x}+v\frac{\partial u}{\partial y}=\frac{\partial^2 u}{\partial y^2}-\rho_s\frac{c_D}{c_{D0}\sigma}(u-u_s),$$

$$u_s\frac{\partial u_s}{\partial x}+v_s\frac{\partial u_s}{\partial y}=\frac{c_D}{c_{D0}\sigma}(u-u_s),\ u_s\frac{\partial v_s}{\partial x}+v_s\frac{\partial v_s}{\partial y}=\frac{c_D}{c_{D0}\sigma}(v-v_s).$$

Here, $x = x'/L$, $y = y'/(L\,\mathrm{Re}^{1/2})$ are dimensionless coordinates (the x axis is directed along the plate, while the y axis is directed normal to the plate; $u = u'/u_\infty$, $v = v'/(u_\infty \mathrm{Re}^{1/2})$ are dimensionless components of velocity in the x and y directions, respectively; $\sigma = \tau_s/(L/u_\infty)$ is the Stokes number, characterizing the intensity of viscous interaction of the phases; $\tau_s = \rho_s^0 d_s^2/18\mu$ is the characteristic relaxation time of particle velocity; μ is the viscosity coefficient of the carrier phase; ρ_s^0 is the physical density of the particles;

Tomsk. Translated from Zhurnal Prikladnoi Mekhaniki i Tekhnicheskoi Fiziki, No. 5, pp. 54-61, September-October, 1987. Original article submitted June 3, 1986.

 0021-8944/87/2805-0692$12.50

d_s is the particle diameter; L is the characteristic dimension (chosen below); $\rho_s = \rho_s'/\rho_\infty$ is the dimensionless continuous density; ρ_∞ is the density of the carrier phase; $Re = \rho_\infty u_\infty L/\mu$ is the Reynolds number of the carrier phase; $c_D = c_D(Re_s)$ is the drag coefficient of the particles; $Re_s = \rho_\infty|v' - v_s'|d_s/\mu$ is the relative Reynolds number; v' and v_s' are the velocity vectors of the phases; $c_{D0} = 24/Re_s$ is the Stokes drag coefficient of the particles; the subscript s pertains to parameters of the particles; the subscript ∞ pertains to undisturbed parameters of the mixture; the primes denote dimensional parameters.

System (1.1) must be solved with allowance for the boundary and initial conditions

$$u(x, \infty) = 1,\ u_s(x, \infty) = 1,\ \rho_s(x, \infty) = \rho_{s\infty}; \tag{1.2}$$

$$\frac{dv_{se}}{dx} = \frac{1}{\sigma}(v_e - v_{se}); \tag{1.3}$$

$$u(x, 0) = 0,\ v(x, 0) = v_w(x); \tag{1.4}$$

$$\rho_s(0, 0) = \rho_{s\infty},\ u_s(0, 0) = 1,\ v_s(0, 0) = 0, \tag{1.5}$$

where $v_e(x)$ and $v_{se}(x)$ are values of the functions v and v_s on the external boundary of the boundary layer; $v_w(s)$ is the specified injection or suction velocity on the surface (the subscript w henceforth corresponds to parameters on the surface of the plate). System (1.1), with boundary conditions (1.2)-(1.4), was obtained by the method of joinable asymptotic expansions [4]. This is in contrast to the method of boundary-layer corrections used in [1].

It should be noted that the boundary condition for the transverse component of particle velocity v_s on the external boundary of the boundary layer (1.3) reflects the effect of interaction of the inviscid external flow and the boundary layer through the velocity component v_s. This condition is an additional equation which must be solved together with system (1.1), since it includes the function v(x, y). This function is not known until the equations of the boundary layer are solved. On the other hand, the boundary-layer equations cannot be solved without knowing the velocity component v_{se} on the external boundary of the boundary layer, which is found from (1.3).

It should be emphasized that since a one-pressure model was used to describe the flow of the two-phase medium in the derivation of system (1.1), this system has the same range of application as the model in [5, 6], strictly speaking. In any case, it can be used to mathematically describe flows in boundary layers for aerosols. It was also assumed that with suction of gas from the surface, particles falling on the surface are removed from the flow region. This assumption may be valid for sufficiently fine or coarse particles.

2. Numerical Solutions of the Equations of a Two-Phase Boundary Layer and Their Analysis. System (1.1), with boundary and initial conditions (1.2)-(1.5), was solved numerically. The equations for the carrier phase were solved by an implicit method [7] having an accuracy on the order of $O(\Delta x^2, \Delta y^4)$. The equations of motion of the disperse phase were solved by Euler's method, with correction along the particle streamlines. The order of accuracy here was $O(\Delta x^2)$. At each step for x, we used iteration to match the values of the parameters of the gas and condensed phases. Here, the equations of the carrier phase were converted to parabolic variables x, η ($\eta = y/\sqrt{2x}$), and we wrote the following for the stream function:

$$f(x, \eta) = f_w + \int_0^\eta u d\eta', \quad v = \frac{1}{\sqrt{2x}}\left[\int_0^\eta \eta u_\eta d\eta - (f_w + 2x f_x)\right],$$

from which the boundary condition for the stream function has the form $f_w \equiv f(x, 0) = -v_w\sqrt{2x}$. In performing the numerical calculations, the characteristic dimension L was chosen to be equal to the relaxation length of particle velocity, $L = u_\infty(\rho_s^0 d_s^2/18\mu)$.

The behavior of the solution for a stationary and impermeable plate surface with a Stokes law of particle drag was studied in sufficient detail in [2]. Here, we present results for this problem when the particle drag coefficient in the gas is given by a formula [8] which more closely reflects reality and adequately describes the experimental data at $0 \le Re_s \le 1000$. Then the expression for c_D/c_{D0}, entering into (1.5), can be transformed:

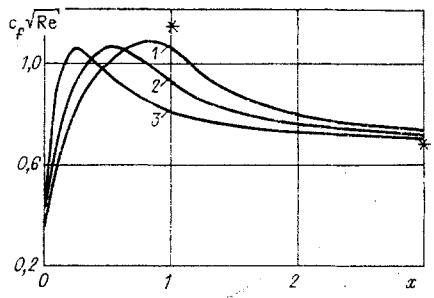

Fig. 1

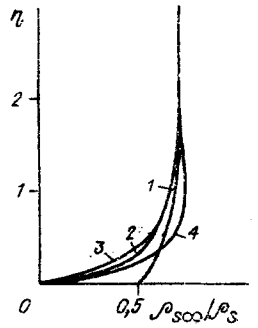

Fig. 2

$$\frac{c_D}{c_{D0}} = 1 + \frac{1}{6}\mathrm{Re}_s^{2/3} = 1 + \frac{1}{6}\mathrm{Re}_{s\infty}^{2/3}|u - u_s|^{2/3} \qquad (2.1)$$

$$(\mathrm{Re}_{s\infty} = \rho_\infty u_\infty d_s/\mu = \mathrm{Re}\, d_s/L).$$

In accordance with the notion of continuity of the gas and particles and the estimate for the thickness of the two-phase boundary layer $O(\mathrm{Re}^{-1/2})$, we obtain an estimate of the upper bound for the criterion $\mathrm{Re}_{s\infty}$ in Eq. (2.1):

$$\mathrm{Re}_{s\infty} \ll \mathrm{Re}^{1/2}.$$

In the case of flow about a spherical particle, the maximum Reynolds number Re achievable for laminar flow is about $2\cdot10^5$. Thus, the condition $\mathrm{Re}_{s\infty} \ll 450$ should be satisfied for laminar flow in the boundary layer.

Figure 1 shows values of the local coefficient of viscous drag $c_f^{(\mu)}\sqrt{\mathrm{Re}}$ on the plate surface, where $c_f^{(\mu)} = \mu(\partial u'/\partial y')/(\rho_\infty u_\infty^2)$, for $\rho_{s\infty} = 3$ and $\mathrm{Re}_{s\infty} = 0$, 10, and 100 (curves 1-3). This situation corresponds physically to an increase in particle size with a simultaneous increase in the characteristic particle stagnation length. For an impermeable plate surface, there is no friction due to particle interaction with the surface. It is evident from a comparison of the results in Fig. 1 that with an increase in particle size due to inclusion of the nonlinear term in the drag coefficient in Eq. (2.1), the dimensionless coordinate of the drag coefficient maximum on the plate is shifted toward the forward critical point by a factor of more than two compared to curve 1, obtained with a Stokes resistance law. This occurs because the particles in the boundary layer begin to be slowed more intensively, and a layer of higher particle density is formed at lower values of the dimensionless coordinate x. It is interesting to note that there is some reduction in the value of the maximum of $c_f^{(\mu)}\sqrt{\mathrm{Re}}$ with an increase in particle size. With an increase in x, all of the curves in Fig. 1 approach a single limiting value equal to $(c_f\sqrt{\mathrm{Re}})_0\sqrt{1 + \rho_{s\infty}}$, where $(c_f\sqrt{\mathrm{Re}})_0 = 0.332$ is the Blasius value of the friction coefficient [9].

The asterisk in Fig. 1 shows results of the numerical solution for the Stokes law of particle drag [2], the difference from our results being 9% in the region of the maximum of c_f. This is evidently due to high values of the density of the disperse phase near the plate surface obtained in [2]. In fact, from (1.1) for a Stokes particle-drag law, we have the following along the particle trajectory at $\varepsilon \ll x < \sigma - \varepsilon$ ($\varepsilon \ll 1$ is the distance from the sample trajectory being examined to the plate surface at the entry point of the boundary layer)

$$\begin{aligned} u_s(x, \varepsilon) &= 1 - \sigma^{-1}x + O(\varepsilon), \\ v_s(x, \varepsilon) &= k(1 - \sigma^{-1}x)\varepsilon + O(\varepsilon^2), \\ y_s(x, \varepsilon) &= (1 + kx)\varepsilon + O(\varepsilon^2), \\ \rho_s(x, \varepsilon) &= \rho_{s\infty}/[(1 - \sigma^{-1}x)(1 + kx\sigma^{-1})] + O(\varepsilon), \end{aligned} \qquad (2.2)$$

where $k = 1$ is a constant determined through combination with the analogous solution in the region $x \sim O(\varepsilon^2)$. It is evident from the last equation of (2.2) that $\rho_{sw} \neq \rho_{s\infty}/u_{sw}$, as in [2]. Meanwhile, this quantity is considerably smaller in value due to the displacing effect of the boundary layer. The results of asymptotic solution (2.2) agree well with numerical solutions.

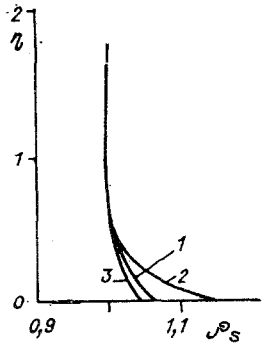

Fig. 3

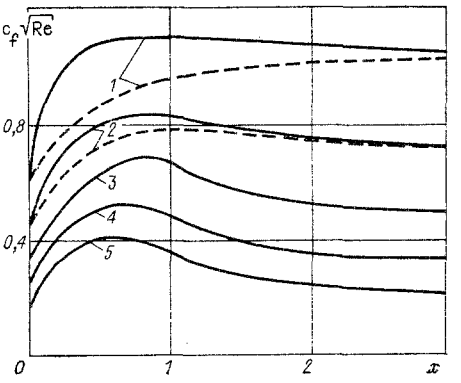

Fig. 4

Figure 2 shows profiles of the density of the disperse phase calculated at $\rho_{s\infty} = 3$, $Re_{s\infty} = 100$, and x = 0.1, 0.4, 1, and 10 (curves 1-4). The value of ρ_s increases along the particle trajectory due to deceleration of the disperse phase before relaxation of the longitudinal components of phase velocity. The value of ρ_s then decreases due to an increase in particle velocity above the velocity of the carrier phase in the transverse direction. The longitudinal components of velocity of the phase remain nearly the same. The difference in transverse velocities results in the appearance of a minimum of ρ_s (Fig. 2, profile 4). The value of ρ_s remains constant along the trajectory at large values of x. With a fixed coordinate η, an increase in x is accompanied by an initial increase in the density of the disperse phase and then a decrease in same. It should be noted that the thickness of the layer of high density ρ_s in the case of a nonlinear drag law for $Re_{s\infty} = 100$ is greater (by a factor of about two) than for the Stokes drag law. This can be attributed to the more intensive deceleration of the particles. The behavior of the profiles of velocities u, u_s, v, and v_s is qualitatively the same as in the case of the Stokes drag law studied in detail in [2]. However, at the value of c_D determined by Eq. (2.1), there is a more rapid equalization of velocities.

Let us examine a two-phase boundary layer in the presence of suction of gas from the plate surface. Here and below, for the sake of simplicity we will assume the existence of a Stokes particle-drag law. We will also assume that the suction (injection) parameter is constant along the plate surface, f_w = const. The behavior of the velocity profiles is qualitatively similar to the case of flow over an impermeable surface, the only difference being that the longitudinal velocity of the particles on the surface does not vanish at finite values of x but instead approaches zero with an increase in x. The normal components of the velocity of the particles and carrier phase on the plate surface are also nontrivial, and the condition $|v_{sw}| < |v_w|$ is satisfied. We should also note the faster relaxation of the normal components of phase velocity compared to the tangential components.

Figure 3 shows profiles of the density of the disperse phase in the sections x = 0.4, 2, and 20 (curves 1-3) calculated with $f_w = 0.5$ and a continuous particle density in an undisturbed flow $\rho_{s\infty} = 1$. It is evident that ρ_s has a finite maximum value on the plate surface. The density of the disperse phase on the surface initially increases with an increase in x as a result of particle deceleration and then decreases very slowly. The latter is connected with the fact that, at high values of x, ρ_s remains nearly constant along the particle trajectory but the particles stay in the boundary layer for a fairly long time before falling to the surface. Thus, for the example shown in Fig. 3, a particle located in the boundary layer at x = 0.15 falls onto the plate only at x = 10. In the limit at $x \to \infty$, the density of the disperse phase approaches uniformity and $\rho_s \to \rho_{s\infty}$. It should be noted that the phenomenon of the reduction in ρ_s at high x is nearly absent due to the small difference in the transverse velocity components of the phases. Suction diminishes the thickness of the high-density layer and significantly reduces the density of the disperse phase in the boundary layer. As a result of the impact of particles on the plate surface with gas suction, the friction coefficient acquires an additional term

$$c_f = c_f^{(\mu)} + c_f^{(s)}, \qquad (2.3)$$

where $c_f^{(s)}$ is the component due to interaction of the condensed phase with the surface. In the case of a perfectly inelastic particle impact against the plate surface, we have $c_f^{(s)} = \frac{(\rho_s' u_s' | v_s' |)_w}{\rho_\infty u_\infty^2} = \mathrm{Re}^{-1/2} \rho_{sw} | v_{sw} | u_w$.

Figure 4 shows values of the friction coefficient on the surface $c_f\sqrt{\mathrm{Re}}$ calculated from (2.3) with different values of the suction and injection parameter at $\rho_{s\infty} = 1$. Curve 3 corresponds to an impermeable surface, curves 1, 2, 4, and 5 correspond to $f_w = 0.5$, 0.2, −0.2, and −0.4, and the dashed lines show the corresponding coefficients of viscous drag $c_f^{(\mu)}$. It is evident from a comparison of the results that a low suction velocity has only a slight effect on the qualitative behavior of the viscous drag coefficient $c_f^{(\mu)}$ (dashed line 2). However, with a further increase in suction velocity, the maximum value of the coefficient is reached only at sufficiently high values of x (dashed line 1), where phase velocity relaxation begins. This occurs because the suction of the gas and particles of the condensed phase prevents the formation of a layer of high particle density with $\rho_s >> \rho_{s\infty}$.

Due to collisions of the particles with the surface, $c_f^{(s)}$ increases from zero to the maximum value and then again decreases to zero with a further increase in x. Meanwhile, the maximum of $c_f^{(s)}$ is somewhat in advance of the maximum of $c_f^{(\mu)}$. This is to be expected, since $c_f^{(s)}$ takes its maximum value in the region of inertial motion of the particles, while $c_f^{(\mu)}$ becomes maximal in the particle stagnation zone. With gas injection (curves 4 and 5), $c_f^s = 0$, while $c_f^{(\mu)}$ decreases with an increase in $|f_w|$.

It follows from the results obtained here that allowing for the collision of particles with the surface has a significant effect on the drag coefficient and leads to an increase in its local values by up to 25% (curves 1). However, viscous drag remains the determining factor. It should be noted that with an increase in the density of the disperse phase in the incoming flow, the effect of friction due to particle collision with the surface also increases.

Let us discuss the results obtained with gas injection into a two-phase boundary layer from the plate surface. The numerical results show that a particle-free zone is formed near the plate surface. Also, the particle trajectories intersect near the separating streamline at a certain distance from the front edge of the plate, approximately at x (dimensionless) equal to 1.5. The reason for the intersection of particle trajectories is the motion of the particles in the "convergent" velocity field of the carrier phase near the separating streamline of the particles in the region where particle velocity relaxation is appreciable (here, the velocity field is "convergent" in the sense that the velocity vectors at two adjacent points lying on a normal to the plate surface are directed toward each other). The intersection of the particle trajectories will be modeled by a so-called sheet [10], i.e., by a surface of discontinuity having a finite surface density, momentum, etc. As regards the structure of the sheet, we will use assumptions similar to those made in [10]: the thickness of the sheet is small compared to the thickness of the boundary layer; particles falling on the sheet acquire its velocity; the parameters of the sheet do not change through its thickness.

We will write the equations satisfied on a stationary sheet in a boundary layer. With allowance for the estimates in the boundary layer, we have the following, similar to [10, 11]:

$$\frac{dR_{s\lambda}u_{s\lambda}}{dx} = j_{sn}^+, \quad R_{s\lambda}u_{s\lambda}\frac{d\mathbf{v}_{s\lambda}}{dx} = R_{s\lambda}\mathbf{f}_{s\lambda} + j_{sn}^+(\mathbf{v}_s^+ - \mathbf{v}_{s\lambda}),$$
$$[v_n] = 0, \quad [p] = 0, \quad \left[\frac{\partial u}{\partial y}\right] = v_n[u] + R_{s\lambda}f_{s\lambda,x}, \quad [u] = 0. \tag{2.4}$$

Here, $R_{s\lambda} = R_{s\lambda}'\mathrm{Re}^{1/2}/(\rho_\infty L)$ is the dimensionless surface density of particles on the sheet; $v_{s\lambda} = v_{s\lambda}'/u_\infty$ is the dimensionless velocity vector of the sheet particles, $j_{sn}^+ = j_{sn}'/(\rho_\infty u_\infty)$ is the dimensionless flow of particles onto the sheet along a normal to the latter from the direction of the dust-laden gas; $\mathbf{v}_s^+ = \mathbf{v}_s^{+\prime}/u_\infty$ is the velocity vector of the particles with approach toward the sheet from the direction of the dust-laden gas; the brackets denote discontinuities of the variables on the sheet; $\mathbf{f}_{s\lambda} = \mathbf{f}_{s\lambda}'L/u_\infty^2$ is the dimensionless force exerted by the gas on the sheet; v_n is the projection of the velocity vector on the normal to the sheet.

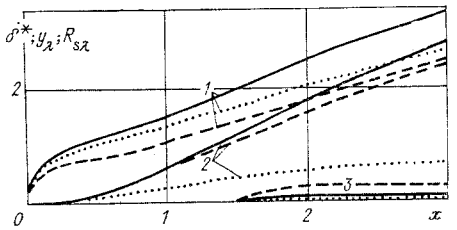

Fig. 5

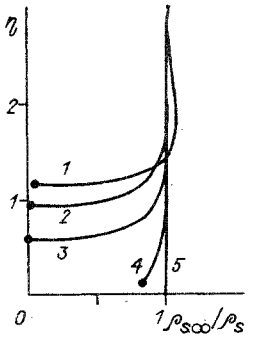

Fig. 6

The last condition in (2.4) follows from estimates of the velocity component u from the equations of motion of the carrier phase inside the sheet with the assumption of a finite value of $\partial u/\partial y$ and a small sheet thickness (compared with the thickness of the boundary layer). This condition is necessary for an unambiguous transition across the surface of discontinuity.

In actual calculations, the first point on the separating streamline where particle trajectories intersect is considered to be the point of origin of the sheet; then we examine Eqs. (2.4) along with Eqs. (1.1). The drag coefficient for the sheet in the first approximation is assumed to be the same as for single spherical particles. As the results of the calculations show, it hardly makes sense to introduce other, more complicated representations for the given problem in light of the relatively small effect of the sheet on the motion of the carrier phase.

Figure 5 shows the dimensionless displacement thickness $\delta^* = \int_0^\infty (1-u)\,dy$, the separating streamline of the particles y_λ, and the surface density of the sheet along the plate (curves 1-3, respectively). The solid lines show results for $\rho_{s\infty} = 1$ and $f_w = -0.4$; the dashed lines show results for $\rho_{s\infty} = 3$ and $f_w = -0.4$; and the dot–dash lines give results for $\rho_{s\infty} = 1$ and $f_w = -0.2$. It was found that the separating streamline, dividing the pure gas from the dust-laden gas, moves away from the plate surface with an increase in injection (curves 2) and approaches the surface with an increase in the density of the disperse phase in the incoming flow. It is interesting to note that the presence of particles has a greater effect on the displacement thickness of the boundary layer than on the thickness of the region of pure injected gas. It was also found that a sheet forms in the region of greatest particle stagnation (curves 3). An increase in injection and the density of the disperse phase in the undisturbed flow is accompanied by an increase in the surface density of the sheet (and, thus, its thickness) and a moderate shift in the stagnation point upstream. With an increase in x, the surface density of the sheet increases to approximately x = 3 (curves 3). With a further increase in x, particle flow onto the sheet nearly ceases, and the surface density of the sheet decreases somewhat due to the low rate of increase in sheet velocity. It should be noted that the velocity of the sheet is lower than the velocity of the gas, i.e., the sheet retards the carrier phase. This in turn reduces the drag coefficient on the plate surface.

Figure 6 shows the behavior of profiles of the density of the disperse phase in the boundary layer at $f_w = -0.4$ and $\rho_{s\infty} = 3$. The value of $\rho_{s\infty}/\rho_s$ is plotted off the x axis. Curves 1-5 correspond to x = 6, 3, 1.4, 0.4, and 0. The points denote the position of the separating streamline. The disperse phase is absent at lower values of the coordinate η. It is evident that the density of the disperse phase near the separating streamline increases with an increase in x and becomes infinite at the unique stagnation point of the sheet (curve 3). With a further increase in x, density ρ_s decreases, taking large values near the sheet (curves 4 and 5). With sufficiently large x in the region where relaxation of the longitudinal components of velocity is substantial, the density of the disperse phase remains constant along the particle trajectory, while a zone of reduced density ρ_s (curve 5) is formed in the external part of the boundary layer because the transverse particle velocity exceeds the transverse velocity of the carrier phase as the longitudinal velocity components are nearing complete relaxation. With an increase in x, the thickness of the high-density layer decreases considerably.

LITERATURE CITED

1. V. P. Stulov, "Equations of a laminar boundary layer in a two-phase medium," Izv. Akad. Nauk SSSR, Mekh. Zhidk. Gaza, No. 1 (1979).
2. A. N. Osiptsov, "Structure of the laminar boundary layer of a disperse mixture on a flat plate," Izv. Akad. Nauk SSSR, Mekh. Zhidk. Gaza, No. 4 (1980).
3. Yu. M. Tsirkunov, "Effect of a viscous boundary layer on particle deposition in the flow of a gas suspension about a sphere," Izv. Akad. Nauk SSSR, Mekh. Zhidk. Gaza, No. 1 (1982).
4. M. Van Dyke, Perturbation Methods in Fluid Mechanics, Parabolic Press (1975).
5. L. A. Klebanov, L. E. Kroshilin, et al., "Hyperbolicity, stability, and correction of a Cauchy problem for the system of equations of two-velocity motion of two-phase media," Prikl. Mat. Mekh., 46, No. 1 (1982).
6. A. N. Kraiko, "Two-fluid model of the flow of a gas and particles dispersed in the gas," Prikl. Mat. Mekh., 46, No. 1 (1982).
7. I. V. Petukhov, "Numerical calculation of two-dimensional flows in a boundary layer," in: Numerical Methods of Solving Differential and Integral Equations and Quadrature Formulas [in Russian], Nauka, Moscow (1964).
8. V. M. Voloshchuk, Introduction to the Hydrodynamics of Coarsely-Dispersed Aerosols [in Russian], Gidrometeoizdat, Leningrad (1971).
9. H. Schlichting, Boundary Layer Theory, 7th ed., McGraw-Hill (1979).
10. A. N. Kraiko, "Surfaces of discontinuity in a medium devoid of internal pressure," Prikl. Mat. Mekh., 43, No. 3 (1979).
11. G. A. Tirskii, "Conditions for surfaces of nonremovable discontinuity in a multicomponent mixture," Prikl. Mat. Mekh., 25, No. 2 (1961).

INFLUENCE OF AN ABRUPT CHANGE IN THE THERMAL BOUNDARY CONDITIONS ON THE TURBULENT BOUNDARY LAYER ON A PLATE

L. N. Drozdova and A. L. Sorokin

UDC 532.526

The development of the thermal boundary layer within a dynamic layer that has already been formed is a situation that is often encountered in the practice of analyzing heat exchangers. The formulation of this problem is represented schematically in Fig. 1. A homogeneous thermal flux q_w acts on a plate with section $x = x_0$ (x_0 is the length of the unheated section), or the surface temperature changes to T_w by a "jump." Here δ_0 is the thickness of the dynamic boundary layer in the section of the "jump," L is the length of the heat transfer section, and u_e and T_e are the rate and temperature of the main flow. The flow is quasiisothermal. This problem is solved by integral methods in [1, 2]. But this approach is inadequately general since it requires additional empirical information. Moreover, it is difficult to obtain a detailed flow pattern by the integral method.

The Patankar–Spalding finite-difference method of solving the system of boundary layer differential equations is used in this paper to solve the formulated problem. The method underestimates the value of the Stanton number St, especially near the section $x = x_0$, where the discrepancy between the experimental results and a computation is about 40% for the data from [2] and about 15% for data from [3].

The method mentioned was also applied by other authors [4] to solve an analogous problem. They visibly experienced similar difficulties since they selected the turbulent Prandtl number Pr_T over the boundary layer section to obtain agreement between experiment and theory in the "jump" zone. The computation was performed with the variable

$$\mathrm{Pr}_{\mathrm{T}}(y) = \frac{\varkappa\left[1-\exp\left(-y/A\right)\right]}{\varkappa_k\left[1-\exp\left(-y/B\right)\right]^2}, \qquad (1)$$

Novosibirsk. Translated from Zhurnal Prikladnoi Mekhaniki i Tekhnicheskoi Fiziki, No. 5, pp. 61-63, September-October, 1987. Original article submitted June 9, 1986.

 0021-8944/87/2805-0698$12.50